Rapid and Slow Voltage-Dependent Conformational Changes in Segment IVS6 of Voltage-Gated Na^+ Channels

Vasanth Vedantham* and Stephen C. Cannon*†‡

*Program in Neuroscience, Division of Medical Sciences, and †Department of Neurobiology, Harvard Medical School; and ‡Department of Neurology, Massachusetts General Hospital, Boston, Massachusetts 02114 USA

ABSTRACT Mutations in segment IVS6 of voltage-gated Na^+ channels affect fast-inactivation, slow-inactivation, local anesthetic action, and batrachotoxin (BTX) action. To detect conformational changes associated with these processes, we substituted a cysteine for a valine at position 1583 in the rat adult skeletal muscle sodium channel α-subunit, and examined the accessibility of the substituted cysteine to modification by 2-aminoethyl methanethiosulfonate (MTS-EA) in excised macropatches. MTS-EA causes an irreversible reduction in the peak current when applied both internally and externally, with a reaction rate that is strongly voltage-dependent. The rate increased when exposures to MTS-EA occurred during brief conditioning pulses to progressively more depolarized voltages, but decreased when exposures occurred at the end of prolonged depolarizations, revealing two conformational changes near site 1583, one coupled to fast inactivation, and one tightly associated with slow inactivation. Tetraethylammonium, a pore blocker, did not affect the reaction rate from either direction, while BTX, a lipophilic activator of sodium channels, completely prevented the modification reaction from occurring from either direction. We conclude that there are two inactivation-associated conformational changes in the vicinity of site 1583, that the reactive site most likely faces away from the pore, and that site 1583 comprises part of the BTX receptor.

INTRODUCTION

Conformational changes in the α-subunit of voltage-gated Na^+ channels are responsible for gating the ion-conducting pore. For example, movement of S4 segments transfers gating charge and confers voltage-dependence upon activation and fast-inactivation (Cha et al., 1999; Yang et al., 1996; Yang and Horn, 1995), and burial of a hydrophobic cluster of amino acids on the III-IV linker is associated with fast inactivation (Kellenberger et al., 1996; Vedantham and Cannon, 1998). Some data suggest that movements in the pore region are related to slow inactivation (Benitah et al., 1999; Todt et al., 1999), while movements associated with the activation gate have not yet been identified.

Recently, evidence has accumulated that a number of gating processes, as well as receptors for pharmacological agents, involve the transmembrane segment IVS6. Site-directed mutagenesis and substituted cysteine accessibility studies have identified regions in this segment that are important for fast inactivation (Cannon and Strittmatter, 1993; Derra et al., 1999; McPhee et al., 1994, 1995), slow inactivation (Hayward et al., 1997; Wright et al., 1998), local anesthetic action (Ragsdale et al., 1994), and batrachotoxin (BTX) action (Linford et al., 1998; Wang and Wang, 1999). In addition, relative movements of S6 segments and their homologs in K^+ channels are believed to underlie activation gating (Liu et al., 1997; Perozo et al., 1999).

In light of this evidence, segment IVS6 is a promising region within which to screen for gating-associated conformational changes, an understanding of which will ultimately be integrated into models of how the parts of Na^+ channels move during gating. As a first step in this process, we have applied the substituted cysteine accessibility method to a residue roughly in the middle of IVS6 in the rat adult skeletal muscle sodium channel α-subunit (rSkM1). Our strategy was to construct the V1583C mutation, express the mutant Na^+ channels in *Xenopus* oocytes, and measure the dependence of the reaction rate of V1583C with methanethiosulfonate (MTS) reagents on voltage, gating, and pharmacological agents. Changes in reaction rate are taken to reflect changes in accessibility of the reactive site, and hence to report either conformational changes or position within the electric field.

We found that the reagent MTS-EA modifies V1583C by causing a reduction in peak current when applied either extracellularly or intracellularly. Our measurements of the modification rate under various conditions are best explained by the hypotheses that the reactive site of V1583C lies within the membrane electric field, probably does not face the pore, upon depolarization undergoes an accessibility increase due to a rapid conformational change, becomes buried as a result of slow inactivation, and either overlaps or is very close to the BTX receptor.

MATERIALS AND METHODS

Mutagenesis and mRNA preparation

We began with the rat skeletal muscle Na^+ channel α-subunit cDNA (rSkM1) containing the IFM1303QQQ mutation and a silent *Cla*I site at base 3865 (Hayward et al., 1996) in the *Xenopus* oocyte expression vector pGEMHE (Liman et al., 1992). Mutation V1583C was engineered into the

Received for publication 9 December 1999 and in final form 7 March 2000.

Address reprint requests to Dr. Stephen Cannon, EDR413A, Massachusetts General Hospital, Boston, MA 02114. Tel.: 617-724-3531; Fax: 617-726-3926; E-mail: cannon@helix.mgh.harvard.edu.

0006-3495/00/06/2943/16 $2.00

construct using the Transformer Site-Directed Mutagenesis Kit (Clontech, Palo Alto, CA), and the region surrounding the introduced mutation was sequenced for confirmation. To generate V1583C in the WT background, a 503-bp *Cla*I-*Sac*II fragment beginning at base 3867 containing the WT sequence at position 1303 was subcloned into the V1583C/IFM1303QQQ construct, thereby replacing QQQ1303 with IFM1303. mRNA for WT rSkM1, V1583C, V1583C/IFM1303QQQ, and human Na^+ channel β_1-subunit (McClatchey et al., 1993) in pGEMHE were all generated by in vitro translation of linearized plasmids with the T7 Message Machine Kit (Ambion, Inc., Austin, TX).

Expression of sodium channels

Harvesting of *Xenopus* oocytes and injection with WT rSkM1 + human β_1 RNA, V1583C + β_1, or V1583C/IFM1303QQQ + β_1 were as described in Chen and Cannon (1995). Between injection and electrophysiological recording, oocytes were incubated for 2–5 days at 18°C in ND-96 (96 mM NaCl, 2 mM KCl, 1.8 mM $CaCl_2$, 1 mM $MgCl_2$, 5 mM HEPES, pH 7.6) supplemented with pyruvate (2.5 mM) and gentamicin (50 μg/ml).

Electrophysiology

Experiments were performed at room temperature after oocytes were manually devitellinized in hypertonic solution. Na^+ currents were measured with an Axopatch 200B amplifier (Axon Instruments Inc., Foster City, CA), whose output was filtered at 5 kHz and digitally sampled at 40 kHz using a Digidata 1200 interface (Axon Instruments Inc.). Data were acquired with a custom AxoBasic data acquisition program and stored on a 75 MHz Pentium-based computer. Leakage conductance and residual capacitance transients were subtracted on-line though digital scaling of passive currents elicited by hyperpolarization from −120 mV to −145 mV.

A two-stage puller (Sutter Instrument Co., Novato, CA) was used to fabricate patch electrodes out of borosilicate capillary tubes (1.65 mm o.d.). The shanks of the pipettes were coated with Sylgard and the tips were heat-polished to a final diameter of 0.5–1.5 μm.

For the inside-out configuration, the pipette solution contained (in mM): 100 NaCl, 10 HEPES, 2 $CaCl_2$, 1 $MgCl_2$, pH 7.6. The bath contained (in mM): 100 KCl, 20 NaCl, 10 HEPES, 5 EGTA, 1 $MgCl_2$, pH 7.6. For the outside-out configuration, these solutions were reversed. One to two milliliters of 40 mM stock solutions in distilled, deionized H_2O of MTS-EA, MTS-ES, MTS-ET, or MTS-HE (Toronto Research Chemicals, Toronto, CA) were made from the solid at the beginning of the recording day and were kept on ice. Appropriate amounts were diluted into 10 ml of bath solution to a final concentration between 0.25 and 2.5 mM after suitable patches had been obtained and immediately before use. MTS solutions were never used for >10 min after dilution from the stock. A patch was included in the study only if the seal formed very rapidly with little or no suction. From previous studies, these conditions produced the most rapid solution exchange kinetics (Vedantham and Cannon, 1998, 1999). Tetraethylammonium chloride (TEA) was obtained from Sigma (St. Louis, MO) and dissolved to 20 mM in either internal or external solution depending on the experiment. BTX, obtained from Dr. Ging Kuo Wang (Brigham and Women's Hospital, Boston, MA) and Dr. John W. Daly (NIDDK, National Institutes of Health, Bethesda, MD), was diluted in electrode solution to a concentration of 5 μM from a 0.5 mM stock in DMSO.

Data analysis

Off-line curve-fitting was performed using SigmaPlot (Jandel Scientific Co., San Rafael, CA), Origin (Microcal, Northampton, MA), or a custom AxoBasic analysis program (Axon Instruments Inc.). Conductance was calculated from raw traces as $G(V) = I_{peak}(V)/(V - E_{rev})$ and fit to a Boltzmann, $G(V) = (G_{max})/(1 + \exp[-(V - V_{1/2})/k])$, where $I_{peak}(V)$ is the peak current at voltage V, E_{rev} is the reversal potential (determined experimentally for each patch), G_{max} is the maximal conductance, $V_{1/2}$ is voltage at half-maximal conductance, and k is the steepness. Steady-state fast inactivation curves were fit to Boltzmanns with non-zero pedestals, I_0, calculated as $I/I_{peak} = (I - I_0)/(1 + \exp[(V - V_{1/2})/k]) + I_0$, where $V_{1/2}$ is the voltage at half-maximal availability, and k is the slope factor. Modification time courses were fit with single-exponential decays to non-zero plateaus, $F = (1 - F_0) \times \exp[-t/\tau_{mod}] + F_0$, where F is the fraction unmodified, t is the cumulative exposure time, τ_{mod} is the time constant of modification, and F_0 is the plateau. The voltage-dependence of the modification rate was fit to a Boltzmann multiplied by an exponential to factor in state-dependence and intrinsic electric field dependence, $R(V) = (R_{min} + (R_{max} - R_{min})/(1 + \exp[-(V - V_{1/2})/k])) \times \exp[z\delta V/25.4]$, where R_{min} and R_{max} are the minimum and maximum modification rates factoring out E-field dependence, $V_{1/2}$ is the voltage at which the rate is half of R_{max}, k is the slope, $z\delta$ is the valence of the MTS reagent multiplied by the fractional electric field distance from the inside, and 25.4 mV is the approximate value of RT/F at room temperature.

Data are plotted as mean values with the standard error of the mean (SEM) indicated with vertical bars. Parameter estimates are presented as mean values ± SEM, except for the voltage-dependence of the modification rate (see Figs. 5 and 6). For these fits, data from all modification experiments were pooled and the standard error of the fitted parameters was estimated from the diagonal of the covariance matrix (Origin).

RESULTS

Comparison of WT with V1583C

All experiments were performed in excised macropatches pulled from *Xenopus* oocytes injected with WT rSkM1 + β_1 RNA, V1583C + β_1 RNA, or V1583C/IFM1303QQQ + β_1 RNA. We began by comparing activation and fast-inactivation gating of WT and V1583C. Fig. 1 *A* shows superimposed normalized current traces elicited by depolarization from −120 mV to −20 mV from inside-out macropatches expressing either WT or V1583C channels. By inspection, there is no significant difference between the two traces. Quantitative comparison of the rates of macroscopic current decay as a function of voltage (Fig. 1 *B*), as well as $G(V)$ and steady-state voltage-dependent availability curves (Fig. 1 *C*), revealed no significant differences between WT and V1583C.

Internal or external MTS-EA modifies V1583C

In the first set of modification experiments, we applied MTS reagents either to the intracellular faces of inside-out patches or to the extracellular faces of outside-out patches expressing either WT or V1583C. None of the MTS reagents used had any irreversible effects on the macroscopic currents carried by patches expressing WT channels (at least $n = 3$ for each reagent from either side).

Among V1583C patches, 1.5 mM MTS-EA caused an irreversible decline in the peak current both when applied intracellularly to inside-out patches and extracellularly to outside-out patches. Fig. 2 *A* shows a series of traces elicited from an inside-out V1583C patch between successive 3-s exposures to 1.5 mM MTS-EA. The peak current progres-

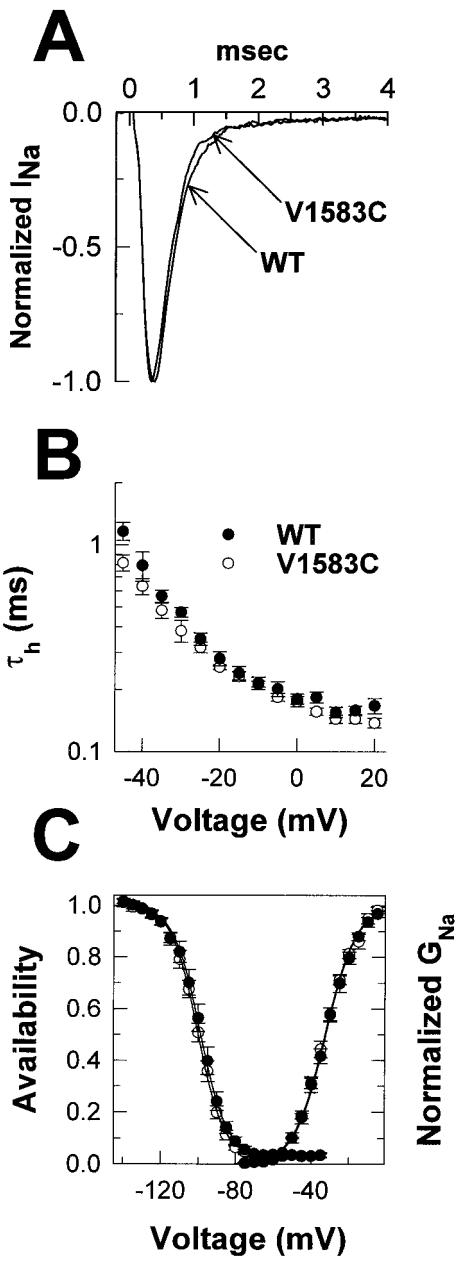

FIGURE 1 Comparison of WT rSkM1 and V1583C: fast gating. (*A*) Current traces were elicited by depolarization from −120 mV to −20 mV from inside-out macropatches expressing either WT rSkM1 or V1583C. One trace from a WT patch and one from a V1583C patch are shown normalized to the peak current and superimposed. (*B*) Current decays from raw traces elicited by step depolarizations from −120 mV to a series of voltages were fit to monoexponentials. The time constants of these fits for V1583C ($n = 4$) and WT ($n = 7$) were plotted against voltage, and showed no significant differences. (*C*) $G(V)$ curves, computed as peak $I_{Na}/(V - E_{rev})$ in response to series of depolarizations from −120 mV were not significantly different for WT ($V_{1/2} = -32.1 \pm 1.1$ mV, slope factor = 8.1 ± 0.1 mV, $n = 7$) and V1583C ($V_{1/2} = -32.7 \pm 0.8$, slope factor = 8.2 ± 0.3 mV, $n = 4$). Steady-state availability curves, measured with 200-ms prepulses to a series of conditioning voltages followed by test pulses to −20 mV, did not differ significantly between WT ($V_{1/2} = -99.0 \pm 1.6$ mV, slope factor = 7.1 ± 0.2 mV, $n = 5$) and V1583C ($V_{1/2} = -100.4 \pm 1.1$ mV, slope factor = 6.9 ± 0.2 mV, $n = 6$).

sively declined, with no apparent change in the shape of the current trace. Fig. 2 *B* shows a series of traces from a similar experiment, with 2-s exposures of outside-out patches to external 1.5 mM MTS-EA (every other trace is shown in the figure). As for intracellular application, extracellular application causes an irreversible progressive reduction in the peak current without a change in macroscopic kinetics.

We estimated the kinetics of the modification reaction by plotting the peak currents from traces elicited between successive exposures against the cumulative exposure time. Fig. 2 *C* shows the resulting modification time course for the data in Fig. 2 *A*, and Fig. 2 *D* shows the time course for the data in Fig. 2 *B*. Each curve was well-fit by a single exponential to a non-zero plateau. After modification was complete, there was generally a small sodium current remaining, slightly greater for extracellular application than for intracellular application (9.3 ± 1.0%, $n = 20$, as compared to 4.0 ± 0.8%, $n = 20$). The reciprocal of the time constant, divided by the concentration of MTS-EA, yields the reaction rate, assuming first-order kinetics. For the curve in Fig. 2 *C*, the rate was 62 $M^{-1}\,s^{-1}$, and for the curve in Fig. 2 *D*, the rate was 50 $M^{-1}\,s^{-1}$.

To check whether the reaction kinetics for internal application of MTS-EA are first-order, we performed the modification reaction at a variety of concentrations of MTS-EA with exposures occurring at −100 mV. Fig. 3 shows a plot of reaction rate (the reciprocal of the time constant) against concentration, with a superimposed linear regression of slope 147 $s^{-1}\,M^{-1}$. The modification rate is roughly linear in concentration, so the reaction appears to be first-order in MTS-EA. In all subsequent experiments, we used 1.5 mM MTS-EA, which lies within the linear range.

In addition to MTS-EA, we attempted modification experiments with MTS-ET, MTS-ES, and MTS-HE. We applied each of these reagents at a concentration of 1.5 mM for 1–2 min at −120 mV, 1–2 min at −20 mV, and during a 1-min series of 10-ms pulses at 40 Hz from −120 mV to −20 mV either intracellularly to inside-out patches or extracellularly to outside-out patches. None of these reagents had any irreversible effects on the shape or peak of the current traces when applied from either direction. To check whether modification had been achieved despite a lack of effects on the current traces, we applied MTS-EA at the end of each experiment and found that full MTS-EA modification could be achieved in every case. This indicates that MTS-ES, MTS-ET, and MTS-HE cannot react with V1583C ($n = 3$ for each experiment).

Two pathways to the reactive site

Previous studies have shown that MTS-EA readily crosses membranes, and so is a poor reporter of the location of reactive thiols relative to the membrane (Holmgren et al., 1996). Thus, despite the fact that we observed modification both with intracellularly and extracellularly applied MTS-

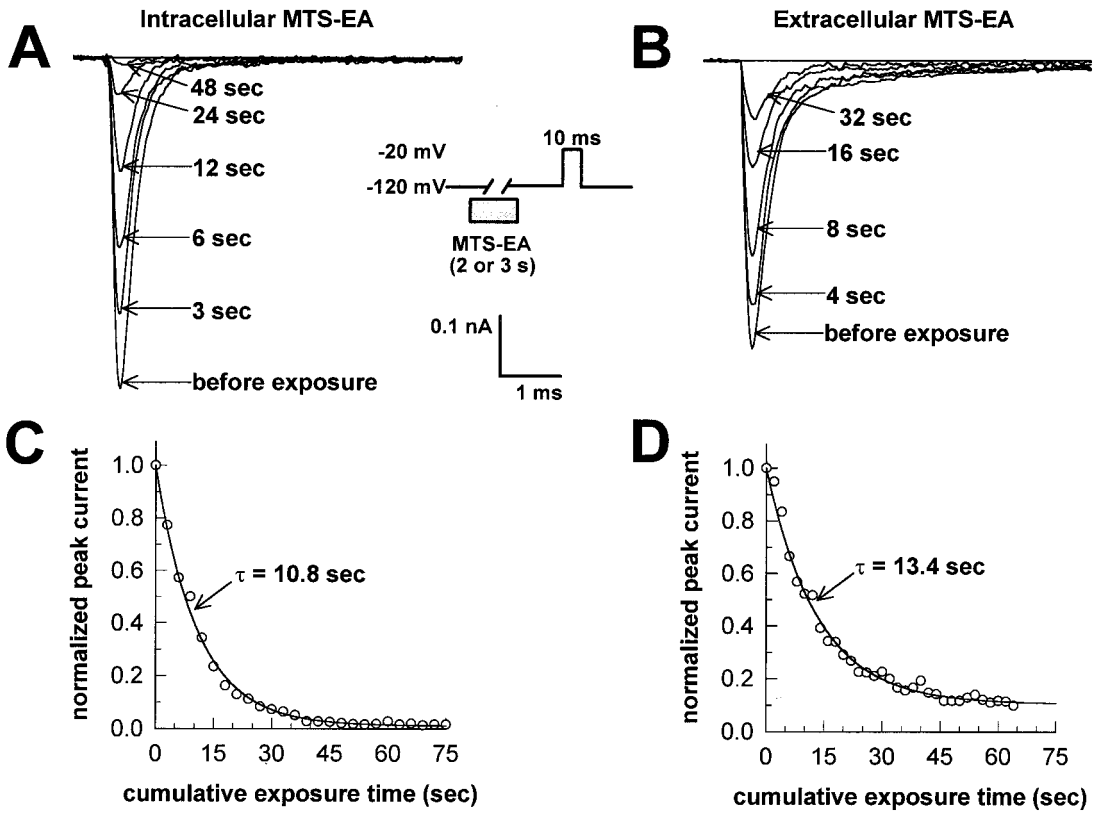

FIGURE 2 Modification of V1583C by internal and external MTS-EA. (*A*) A series of 3-s exposures of the internal face of an inside-out patch to 1.5 mM MTS-EA at −120 mV caused a progressive reduction in the peak currents elicited by test pulses to −20 mV applied between successive exposures (protocol shown between (*A*) and (*B*)). (*B*) A series of 2-s exposures of the external face of an outside-out patch to 1.5 mM MTS-EA at −120 mV also caused a progressive reduction in the peak currents elicited by test pulses to −20 mV applied between successive exposures. (*C*) Peak currents from the experiment shown in (*A*) were plotted as a function of cumulative exposure time, and fit to a single exponential decay with a non-zero plateau. (*D*) Peak currents from (*B*) were plotted as a function of exposure time and fit to a monoexponential decay with a non-zero plateau.

EA, it is possible that the reactive site can only be reached from one side of the membrane, and that modification from the other side occurs because the reagent traverses the membrane, and only then reaches the reactive site. These *trans* effects can be eliminated by adding 20 mM free cysteine, which is membrane-impermeant, to the solution on the side opposite MTS-EA application (Holmgren et al., 1996). To test for the possibility of *trans* effects we performed a set of experiments with free cysteine as a thiol scavenger.

The first experiments, shown in Fig. 4 *A*, were performed with intracellular application of MTS-EA to inside-out patches. As a control experiment, we attempted the modification reaction with both 20 mM cysteine and 1.5 mM MTS-EA on the intracellular side. A plot of the modification time course (*open triangles*) showed no effect of the reagent, as expected because the cysteine rapidly reacts with the available MTS-EA. We then performed the modification experiment with 20 mM cysteine in the electrode solution and 1.5 mM MTS-EA in the bath solution, applied in successive exposures. The mean modification time course over three such experiments (*open squares*) was not different from the mean time course for three experiments without any extracellular cysteine present (*open circles*), demonstrating that there is a modification pathway from the intracellular side to the reactive site that does not require the reagent to completely traverse the membrane.

An analogous set of experiments was performed for extracellular application to outside-out patches (Fig. 4 *B*). The control, in which both cysteine and MTS-EA were included in the extracellular solution, resulted in no modification, as expected (*open triangles*). The experiments in which 20 mM cysteine was added to the electrode solution, and 1.5 mM MTS-EA was applied to the extracellular face (*open squares*), did not result in a mean modification time course significantly different from the experiments with no cysteine present (*open circles*). This demonstrates that extracellularly applied MTS-EA need not traverse the entire membrane to reach the reactive site, and thus there are at least two distinct pathways to the reactive site, one from the extracellular side and one from the intracellular. In addition, the fact that the reaction rates from either side were unaf-

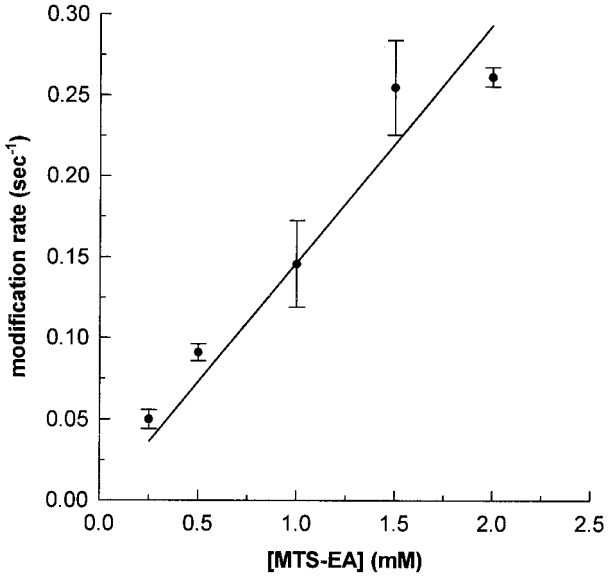

FIGURE 3 Dose-dependence of the reaction rate. Modification rates were measured in inside-out patches at −100 mV with several different concentrations of internal MTS-EA. The dependence of reaction rate on concentration of MTS-EA was roughly linear, with a slope of 147 $M^{-1}\,s^{-1}$.

fected by cysteine demonstrates that the cysteine itself cannot reach the vicinity of the reactive site.

Voltage-dependence of the reaction rate: brief conditioning pulses

In the next set of experiments we explored the voltage-dependence of the modification reaction, both to determine whether there is dependence of reaction rate on rapid voltage-dependent conformational changes and to check for intrinsic electric field dependence. The protocol we used is shown in Fig. 5 *A*. We used a holding potential of −120 mV and timed 50-ms exposures to 1.5 mM MTS-EA to occur in the middle of a 65-ms conditioning pulse. After each exposure, a test pulse was administered to measure the peak current. In the first set of experiments, we applied the MTS-EA intracellularly to inside-out patches at 15 different voltages.

The results exhibit regions of steep and of weak voltage-dependence, consistent with the reaction rate increasing both with a conformational change and with voltage. The curve of modification rate versus voltage shown in Fig. 5 *B* (*filled circles*) was fit to a Boltzmann multiplied by an exponential (see Methods), yielding $R_{max(int)}$ of 1540 ± 53 $M^{-1}\,s^{-1}$, $R_{min(int)}$ of 96.9 ± 62 $M^{-1}\,s^{-1}$, $V_{1/2}$ of −86.8 ± 4.0 mV, slope factor of 9.6 ± 3.0 mV, and $z\delta$ of 0.21 ± 0.03 electric field units. The conformational change causes an increase in accessibility to MTS-EA of ~15-fold.

To test whether this conformational change can be detected by external application of MTS-EA, we repeated

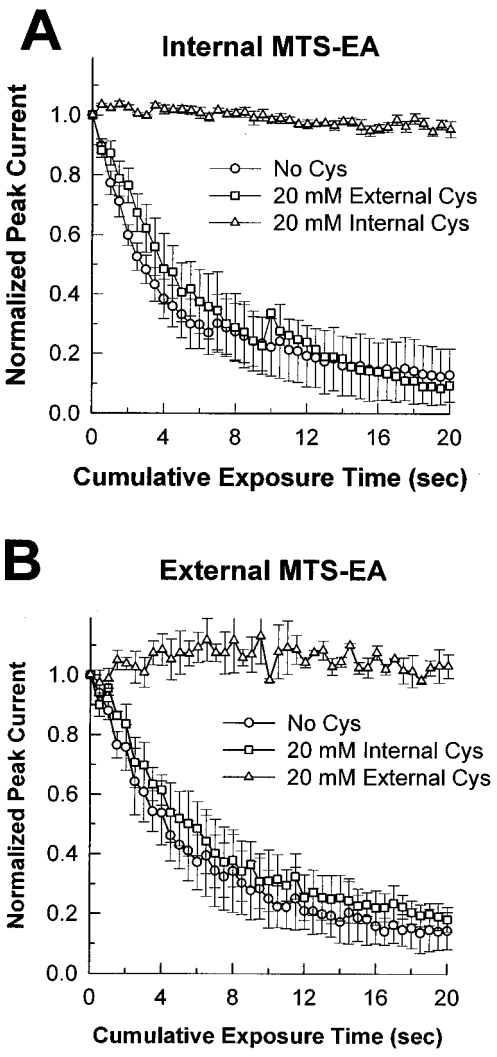

FIGURE 4 Effects of cysteine on MTS-EA modification of V1583C. (*A*) Inside-out patches were given a series of 0.5-s exposures to 1.5 mM MTS-EA at −100 mV, and peak currents elicited by test pulses to −20 mV were plotted against cumulative exposure time either with no cysteine present (*open circles*), 20 mM external cysteine (*open squares*), or 20 mM internal cysteine (*open triangles*). Internal cysteine prevented the modification reaction, while the reaction rate in the presence of 20 mM external cysteine (τ = 5.9 ± 1.4 s, n = 3) was not significantly different from control (τ = 3.9 ± 0.5 s, n = 3). (*B*) Outside-out patches were given a series of 0.5-s exposures to 1.5 mM MTS-EA at −100 mV, and peak currents elicited by test pulses to −20 mV were plotted against cumulative exposure time either with no cysteine present (*open circles*), 20 mM internal cysteine (*open squares*), or 20 mM external cysteine (*open triangles*), while the reaction rate with 20 mM internal cysteine (τ = 7.8 ± 2.8 s, n = 3) was not significantly different from control (τ = 5.9 ± 1.6, n = 3).

some of the voltage-dependence measurements with extracellular application of MTS-EA to outside-out patches. Because of the difficulty of forming and maintaining stable outside-out patches, we only used five voltages. The results, shown in Fig. 5 *B* (*open circles*) show state-dependence with little or no intrinsic electric field-dependence. $R_{max(ext)}$

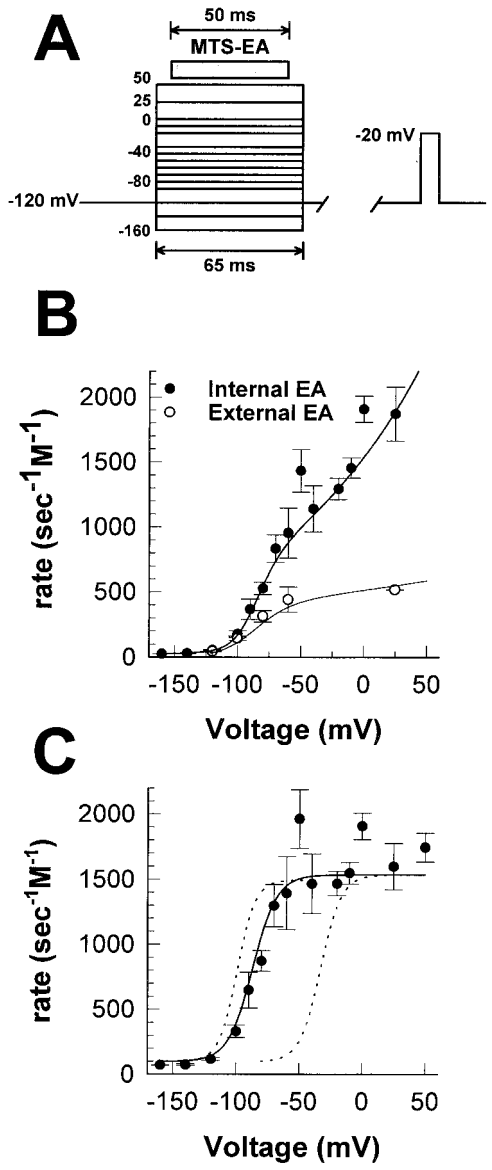

FIGURE 5 Voltage-dependence of the reaction rate: brief depolarizations. (*A*) A series of exposures of inside-out patches to 1.5 mM internal MTS-EA were timed to occur for 50 ms in the middle of a 65-ms conditioning pulse to a specific voltage, enabling us to measure the reaction rate after brief depolarizations at several voltages. Experiments were also performed with outside-out patches and 1.5 mM external MTS-EA at five voltages. (*B*) Reaction rates for internal MTS-EA (*filled circles*) and external MTS-EA (*open circles*) were plotted against conditioning voltage and fit with a Boltzmann multiplied by an exponential $R = (R_{min} + (R_{max} - R_{min})/(1 + \exp[(V_{1/2} - V)/k])) \times \exp[(z\delta V/25.4)]$ to account for state-dependence and intrinsic electric field-dependence. For internal MTS-EA, parameters were $R_{min(int)} = 97 \pm 62\ M^{-1}\ s^{-1}$, $R_{max(int)} = 1540 \pm 53\ M^{-1}\ s^{-1}$, $V_{1/2} = -86.8 \pm 4.0$ mV, $k = 9.6 \pm 3.0$, $z\delta = 0.21 \pm 0.03$. For external MTS-EA, $R_{min(ext)} = 0\ M^{-1}\ s^{-1}$, $R_{max(ext)} = 494 \pm 62$, $V_{1/2} = -89.2 \pm 14.1$ mV, slope factor $= 14.8 \pm 5.2$ mV, and $z\delta = 0.05 \pm 0.10$. (*C*) The data in (*B*) for internal modification were divided by $\exp(0.16V/25.4)$ to compensate for intrinsic E-field dependence and plotted alongside curves of the extent of fast inactivation versus voltage and conductance versus voltage (both data-sets from Fig. 1 *C*), scaled by $R_{max(int)}$ and $R_{min(int)}$. The voltage-dependence of the rapid conformational change lies between the two curves.

was $494 \pm 62\ M^{-1}\ s^{-1}$, $V_{1/2}$ was -89.2 ± 14.1 mV, the slope factor was 14.8 ± 5.2 mV, and the estimated $z\delta$ was 0.05 ± 0.10, though our lack of data at strongly depolarized voltages increases the uncertainty associated with the value for $z\delta$. The minimum reaction rate, $R_{min(ext)}$, was indistinguishable from zero, indicating that when the channel is strongly hyperpolarized there is essentially no accessibility from the outside. The similarity of $V_{1/2}$ from both directions (within 4 mV) suggests that modification from both sides reports a single conformation change that renders the reactive site more accessible to MTS-EA from both sides of the membrane.

Because the exposure was administered during a short conditioning pulse (65 ms), the conformational change tracked by the modification reaction is likely to be one associated with fast gating. To compare the reaction rate data to fast gating behavior obtained from ionic current measurements (from Fig. 1 *C*), the modification rates for internal modification were normalized by the intrinsic voltage-dependence and plotted alongside a curve showing the extent of fast inactivation as a function of voltage and the $G(V)$ curve in Fig. 5 *C*. (Both curves were scaled to $R_{max(int)}$ and $R_{min(int)}$.) The midpoint of the voltage-dependence of the rapid conformational change at site 1583 is 13.6 mV more depolarized than the steady-state voltage-dependent availability curve (-86.8 ± 4.0 mV versus -100.4 ± 1.1 mV), and 54.1 mV hyperpolarized than the $G(V)$ curve (-86.8 ± 4.0 mV versus -32.7 ± 0.8 mV). The lack of close agreement between the voltage-dependence of site 1583 accessibility and either fast inactivation or activation makes the precise role of this transition in voltage-dependent gating unclear.

The $z\delta$ of 0.16 cannot be used to precisely estimate the electrical distance of the reactive site, because MTS-EA might proceed part of the way into the electric field, lose a proton, partition into the membrane, and travel further. (The pK_a of MTS-EA is possibly as low as 8.5 (Holmgren et al., 1996).) Moreover, rapid protonation and deprotonation of MTS-EA might result in a net partial charge, making it difficult to separate the contribution of valence and electric field distance of the reactive site to $z\delta$.

Relation of the rapid conformational change to fast inactivation

Because the voltage-dependence of the modification rate left the nature of the rapid conformational change reported by the reaction unclear, we repeated these measurements on V1583C in the IFM1303QQQ background, which has severely disrupted fast inactivation (West et al., 1992).

Fig. 6 *A* shows modification by successive intracellular exposures to 1.5 mM MTS-EA applied to an inside-out patch expressing V1583C/IFM1303QQQ. As expected, the current before modification shows disrupted fast inactivation. With modification, the peak current is progressively

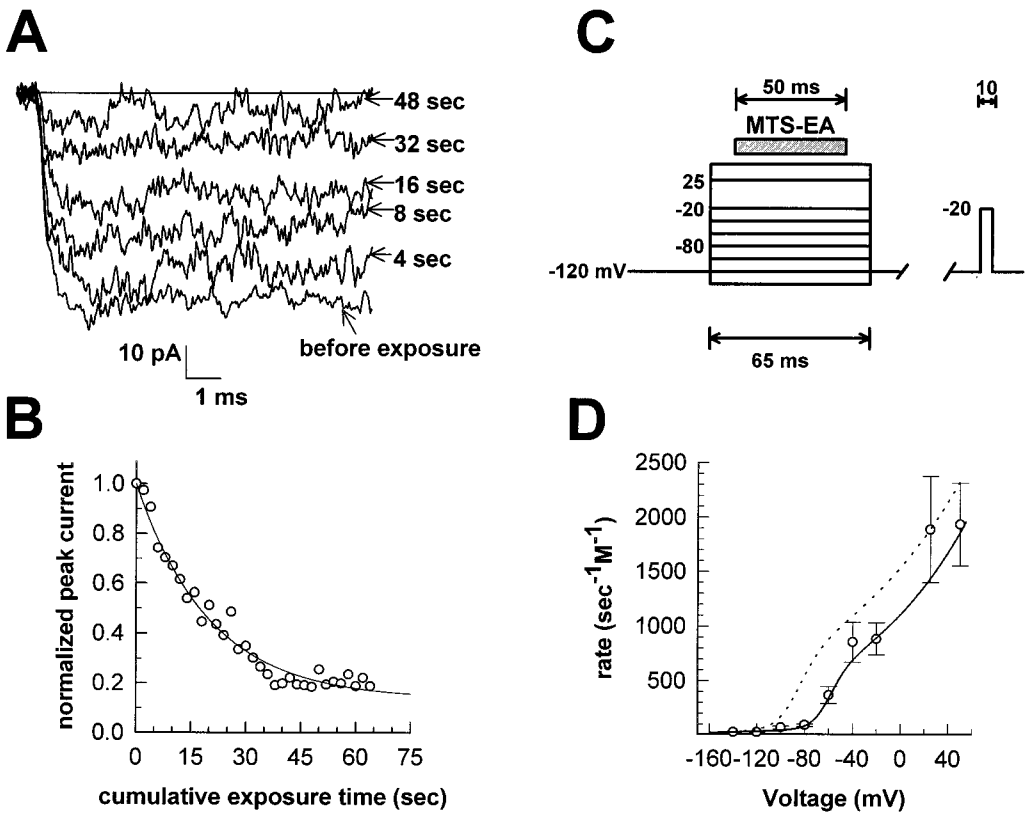

FIGURE 6 Modification of V1583C/IFM1303QQQ. (*A*) An inside-out patch expressing a fast inactivation-deficient version of V1583C was subjected to a series of 4-s exposures to 1.5 mM internal MTS-EA, and showed a progressive reduction in the peak current. (*B*) Peak currents from the experiment shown in (*A*) were plotted against cumulative exposure time, and the curve was fit with a monoexponential curve with a nonzero plateau (τ = 20.1 s, plateau = 13%). (*C*) The protocol used to evaluate the dependence of reaction rate on voltage for V1583C/IFM1303QQQ was identical to that shown in Fig. 5 *A*, except that the reaction rates were measured at fewer voltages. (*D*) Reaction rates measured using the protocol in (*C*) were plotted against exposure voltage (*open circles*). The resultant curve was fit, as in Fig. 5 *B*, with a Boltzmann times an exponential, yielding $V_{1/2} = -60.6 \pm 8.1$ mV, $R_{\min(int)} = 118 \pm 89\ M^{-1}\ s^{-1}$, $R_{\max(int)} = 1107 \pm 118\ M^{-1}\ s^{-1}$, slope factor = 7.8 ± 6.8 mV, $z\delta = 0.26 \pm 0.08$. The dotted line shows the fit to the rate versus voltage curve for V1583C with fast inactivation intact. Loss of fast inactivation appears to shift the voltage-dependence by ~ 26 mV in the depolarizing direction, and slightly depresses $R_{\max(int)}$.

reduced, as is the case with V1583C in the WT background. A plot of peak current against cumulative exposure time (Fig. 6 *B*) is well-fit by a monoexponential decay to a non-zero plateau.

Using the protocol shown in Fig. 5 *A*, we examined the voltage-dependence of the reaction rate at nine voltages. The results, shown in Fig. 6 *D* (*open circles*), indicate that the conformational change of V1583C/IFM1303QQQ reported by the reaction rate occurs at more depolarized potentials than that reported by the rate in V1583C (*dashed line*). A fit to a Boltzmann multiplied by an exponential and comparison to the parameters for V1583C reveals similar minimum rates ($119 \pm 89\ M^{-1}\ s^{-1}$ as opposed to $97 \pm 62\ M^{-1}\ s^{-1}$), a somewhat smaller maximum rate ($1107 \pm 118\ M^{-1}\ s^{-1}$ as opposed to $1540 \pm 53\ M^{-1}\ s^{-1}$), similar slope factors (7.8 ± 6.8 mV as opposed to 9.6 ± 3.0 mV), and similar electric field-dependence (0.26 ± 0.08 as opposed to 0.21 ± 0.03). The greatest change was a depolarizing shift of ~26 mV in the voltage-dependence of the conformational change (−60.6 ± 8.1 mV as opposed to −86.8 ± 4.0 mV).

The fact that the $R_{\max(int)}$ and $R_{\min(int)}$ are not greatly altered in the fast-inactivation defective mutant suggests that the part of the fast-inactivation mechanism contributed by III-IV linker movement is not a necessary condition for the occurrence of the conformational change reported by the reaction, although the modest decrease in $R_{\max(int)}$ might be caused by a reduction in the maximal fraction of channels capable of undergoing the conformational change.

The shift in voltage-dependence, however, is consistent with the idea that the conformational change is coupled to fast inactivation, because more depolarization was required to get the same fraction of channels to undergo the conformational change when fast inactivation was disrupted. Nevertheless, this coupling must be indirect because the IFM1303QQQ mutation completely prevents fast inactivation of ionic current, but only causes a shift in the voltage-dependence of the conformational change. By "coupling"

we do not imply that fast inactivation and the rapid movement at site 1583 have the same or even similar structural or mechanistic bases. Rather, coupling merely implies that fast inactivation influences the propensity of channels to undergo the conformational change tracked by site 1583 accessibility.

Site 1583 is buried during slow inactivation

The preceding experiments were designed to test changes in accessibility of site 1583 associated with rapid gating transitions. In the next set of experiments, we tested the accessibility of site 1583 during the development of slow inactivation in V1583C with fast inactivation intact.

We began by measuring the time course of entry to slow inactivation at −20 mV. Fig. 7 *A* shows the results of a two-pulse protocol. The peak currents elicited by brief test pulses from −120 mV to −20 mV were divided by the peak currents measured after variable length conditioning pulses to −20 mV, with a 50-ms gap at −120 mV to allow recovery from fast inactivation between the conditioning and test pulses. There was little slow inactivation in the first 50 ms, approximately half of the channels became slow-inactivated by 200 ms, and there was nearly complete slow inactivation by 2 s.

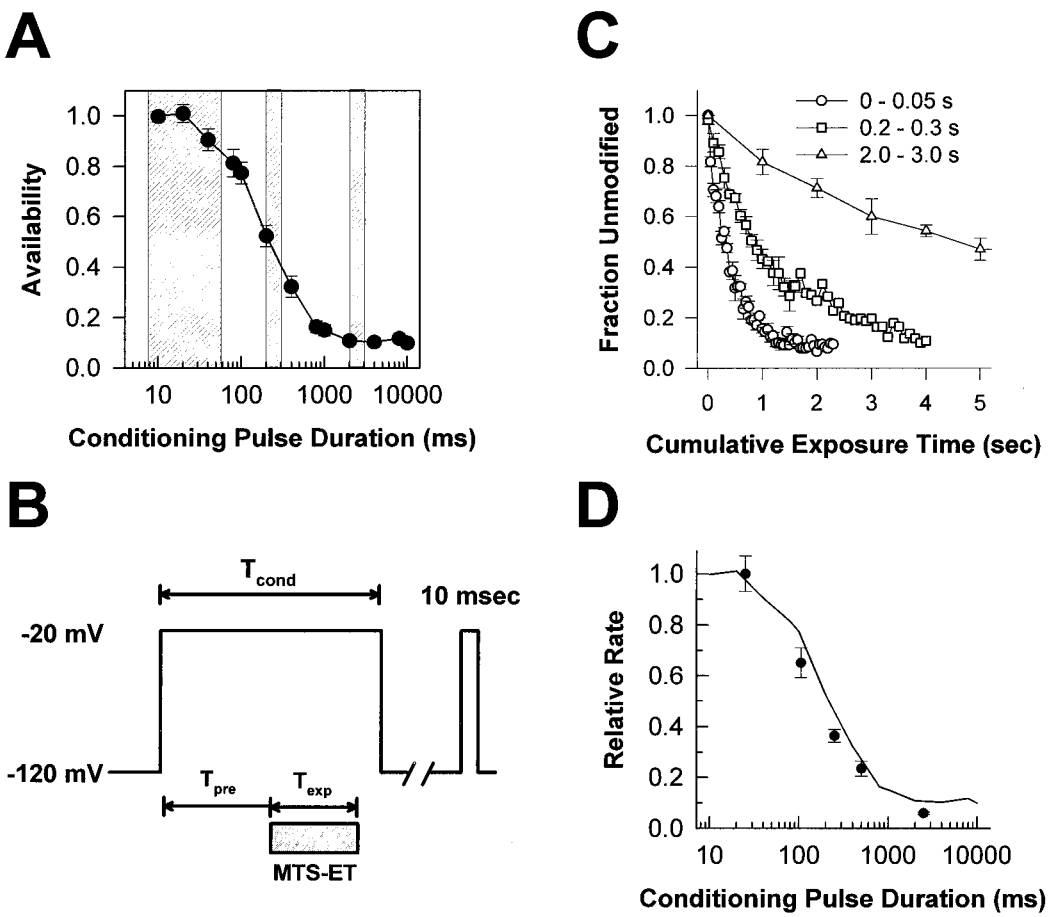

FIGURE 7 Modification rate during long depolarizations. (*A*) A two-pulse protocol was used to measure the rate of entry to slow inactivation for V1583C with fast inactivation intact. A variable-length conditioning pulse from −120 mV to −20 mV was followed by a 50-ms gap at −120 mV to allow recovery from fast inactivation, and a 3-ms test pulse to −20 mV. The peak current from the test pulse was divided by the peak current from the conditioning pulse and plotted against the conditioning pulse duration. (*B*) Exposures were timed to occur at −20 mV for different intervals (T_{exp}) after different durations at −20 mV (T_{pre}) to estimate the change in reaction rate with the development of slow inactivation. (*C*) Series of successive exposures of inside-out patches to 1.5 mM internal MTS-EA at −20 mV were conducted using different-length conditioning pulses. Exposures occurred during intervals with varying degrees of slow inactivation: the first 50 ms of depolarization ($n = 3$), from 200 to 300 ms after depolarization ($n = 4$), or between 2 and 3 s after depolarization ($n = 3$). Depolarizations were maintained during the exposures. These exposure intervals correspond to the shaded area in (*A*). The peak currents from these series of exposures are plotted against cumulative exposure time. The modification rate is slower as the degree of slow inactivation increases. (*D*) The reaction rates at −20 mV for different exposure intervals were divided by the rate for the 0–50-ms exposure interval (1760 ± 122 $M^{-1}\,s^{-1}$, $n = 3$) and plotted against conditioning pulse duration before exposure. The solid circles are plotted at time points at the midpoint of the exposure interval ($T_{pre} + 0.5 \times T_{exp}$): 0–50 ms ($n = 3$), 50–130 ms ($n = 4$), 200–300 ms ($n = 4$), 400–600 ms ($n = 3$), or 2–3 s ($n = 3$) after depolarization. The solid line shows the development of slow inactivation at −20 mV measured for ionic currents, the same data as in (*A*).

The protocol we used to test the accessibility of site 1583 during slow inactivation is shown in Fig. 7 *B*. Internal exposures to inside-out patches occurred within conditioning pulses to −20 mV for variable durations at various times within the conditioning pulse. This way, V1583C would be exposed to 1.5 mM MTS-EA with different fractions of the total population slow-inactivated. Between each conditioning pulse, a period at the holding potential was maintained long enough to allow complete recovery from slow inactivation (14 s) before a test pulse was administered to assay the peak current. Changes in accessibility of V1583C would be reflected in changes in reaction rate from the earliest time points (with little slow inactivation) to later time points (with nearly complete slow inactivation). The shaded areas in Fig. 7 *A* show times and durations of exposures to MTS-EA relative to the fraction of channels slow-inactivated.

Mean time courses from the modification experiments performed using the protocol in Fig. 7 *B*, for exposure times and durations shown in the shaded area of Fig. 7 *A*, are shown in Fig. 7 *C*. These time courses clearly show that as slow inactivation progresses, the rate of modification slows. A more precise comparison of modification rate and extent of slow inactivation is shown in Fig. 7 *D*. Individual modification time courses were fit with exponential decays, and the reaction rate was calculated from the decay time constant. The first time point, measured for exposures that occurred between 0 and 50 ms after depolarization, reflects the rate of modification in the absence of slow inactivation. The rates acquired from experiments with exposures later in the conditioning pulse were normalized by dividing by the 0- to 50-ms time point. The result was the fractional decrease in modification rate with increasing conditioning pulse duration. The rates were plotted against the time at which the exposure reached its midpoint ($T_{pre} + 0.5 \times T_{exp}$), and show a progressive decline to a rate of 104 ± 8 $M^{-1}\,s^{-1}$ ($n = 3$), a fractional decrease of ~17-fold. The solid line in Fig. 7 *D* shows the development of slow inactivation as measured by ionic currents (the same data as in Fig. 7 *A*), and shows that the reduction of modification rate with time closely parallels the development of slow inactivation.

As a more stringent test of this correlation between site 1583 accessibility and slow inactivation, we tested the voltage-dependence of the slow inactivation-associated reduction in reaction rate. The protocol we used is shown in Fig. 8 *A*. Exposures were timed to occur between 2 and 3 s after depolarization within a 3.5-s conditioning pulse. Between each exposure, a test pulse was administered to monitor the progressive reduction in peak current. The resulting modification time courses were fit as before to obtain a reaction rate. These rates were divided by the rates measured at the same voltage when the exposure occurred during the first 50 ms of depolarization (the data from Fig. 5 *B*) to obtain the fractional reduction in rate associated with development of slow inactivation. This fractional reduction corresponds to the fraction of channels that become slow-inactivated after 2.5 s at the conditioning pulse. These normalized reaction rates were plotted as a function of voltage in Fig. 8 *B* (*filled circles*; the point at −120 mV was defined to be 1.0).

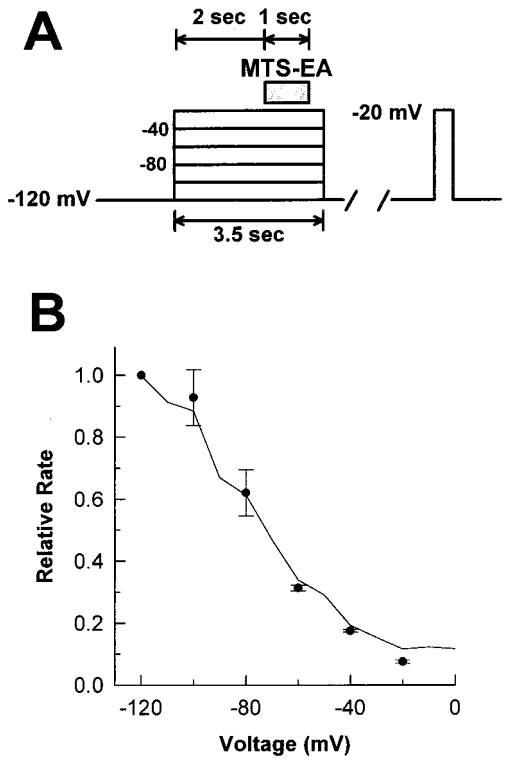

FIGURE 8 Voltage-dependence of slow inactivation-associated changes in modification rate. (*A*) Exposures were timed to occur between 2 and 3 s into 3.5-ms conditioning pulses to different voltages. (*B*) The modification rate measured when exposures were timed to occur between 2 and 3 s into the conditioning pulse were divided by those measured when exposures occurred from 0 to 50 ms for a variety of conditioning voltages (the latter values were taken from the data in Fig. 5 *B*, *filled circles*; the −120 mV ratio was set to 1.0 by definition, as V_h was −120 mV). The resulting curve shows the voltage-dependence of the slow inactivation-associated reduction in the modification rate ($n = 3$ for all points). The solid line shows the fraction of channels slow-inactivated by a 2.5-ms pulse as a function of voltage measured with ionic currents using a two-pulse protocol (V_h = −120 mV, 50 ms gap at V_h).

The solid curve shows data acquired from a two-pulse protocol used to measure the amount of slow inactivation as a function of voltage for a 2.5-s depolarization. Control measurements at −20 mV were followed by 2.5-s conditioning pulses to different voltages which, in turn, were followed by a 50-ms gap at −120 mV and a test pulse to −20 mV. The peak current in the test pulse was divided by the peak current of the control pulse to arrive at the fraction of channels slow-inactivated during the 2.5-ms depolarization.

Because the data showing the voltage-dependence of the fractional reduction in reaction rate agree extremely well with the ionic-current data on the voltage-dependence of

slow inactivation at the 2.5 s time point, we can assert with confidence that the accessibility of site 1583 is a faithful reporter of a conformational change associated with slow inactivation.

The presence of TEA in the pore does not affect the modification rate

The results presented so far have suggested that the accessibility of site 1583 reports a rapid conformational change coupled to fast inactivation, tracks a conformational change associated with slow inactivation, and is nearly equal from either side of the membrane. The latter finding raises the question of the nature of the pathways to the reactive site and, in particular, the position of site 1583 within the channel; i.e., whether the sulfhydryl group modified by MTS-EA faces the pore or faces away from the pore.

To begin to address this question, we measured the reaction rate in the presence of the pore blocker TEA. In cardiac sodium channels, internal TEA blocks sodium channels from the inside at an electric field distance of ~50% (O'Leary and Horn, 1994). Fig. 9 *A* shows the reduction in peak current associated with 20 mM TEA block at +25 mV, ~65%.

To test whether this level of TEA block can affect the internal access pathway of MTS-EA, we measured the modification rate during TEA block. Even if the site of TEA block is further into the pore than the reactive site (as the $z\delta$ of 0.16–0.26 for internal modification suggests), TEA might affect the reaction rate via an electrostatic effect rather than a steric effect. (Both TEA and MTS-EA carry net positive charges.) Fig. 9 *B* shows the effect of 20 mM internal TEA on the modification time courses at +25 mV. The protocol used was that shown in Fig. 5 *A* for +25 mV, with the open circles representing mean time courses with TEA present, and the filled circles representing modification time courses under control conditions. These rates were not significantly different, making it unlikely that MTS-EA travels further than 50% of the way into the E-field from the inside via an aqueous pathway into the pore.

Because both the $z\delta$ measurements and the results with internal modification during TEA block suggest that the reactive site lies further toward the inside than the location at which TEA blocks, internal TEA block should substantially reduce the reaction rate from the outside if the external pathway to the reactive site involves the pore.

Fig. 9 *C* shows experiments with external exposure to 1.5 mM MTS-EA at +25 mV with (*open circles*) and without (*filled circles*) 20 mM internal TEA present. The mean modification time courses for these two conditions were not significantly different, indicating that occupancy of the internal vestibule of the pore by TEA for 65% of the time has no effect on the access pathway to the reactive site from the outside. This renders it very unlikely that the external access pathway is via the pore. More likely, external MTS-EA

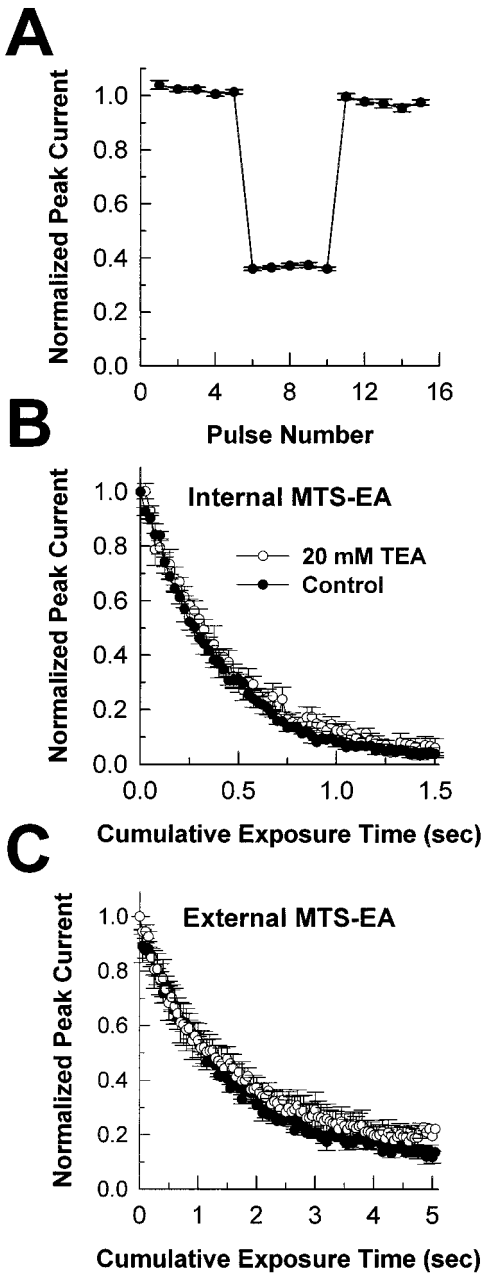

FIGURE 9 Internal TEA does not affect the modification rate. (*A*) Inside-out patches were subjected to a series of 15 depolarizations to +25 mV. For the middle five pulses the patches were transferred to a bath containing 20 mM internal TEA. Peak currents were normalized to the average of the peak current from the 10 traces elicited under control conditions and plotted against pulse number. Peak current was reduced by 63.5 ± 0.3% in the TEA ($n = 6$). (*B*) Inside-out patches were subjected to a series of 50-ms exposures to 1.5 mM MTS-EA at +25 mV with 20 mM internal TEA present (*open circles*) or with no TEA present (*filled circles*). There was no significant difference in the modification time courses measured with TEA (0.41 ± 0.05 s, $n = 3$) or without TEA (0.40 ± 0.03 s, $n = 3$). (*C*) Outside-out patches were subjected to a series of 50-ms exposures to 1.5 mM MTS-EA at +25 mV with 20 mM internal TEA present (*open circles*) or with no TEA present (*filled circles*). The reaction rate for patches with TEA present (1.4 ± 0.3 s, $n = 3$) was not different from control (1.3 ± 0.1 s, $n = 3$).

loses a proton, enters the membrane, and reaches the reactive site by diffusing within the membrane. This hypothesis is consistent with a lack of intrinsic electric field-dependence from the outside, and with the results of the thiol scavenger data, which demonstrated that external MTS-EA doesn't fully traverse the membrane to reach the reactive site.

V1583C is protected from modification by batrachotoxin

Batrachotoxin is a lipophilic activator of sodium channels that shifts the voltage-dependence of activation in the hyperpolarizing direction and prevents the occurrence of both fast and slow inactivation. Mutations at residues near V1583C (N1584 and F1579) dramatically disrupt BTX action (Linford et al., 1998; Wang and Wang, 1999), suggesting that the BTX receptor may be close to V1583. We decided to test this hypothesis by measuring the modification rate in BTX-activated channels. Also, because BTX is lipophilic and is believed to bind to Na^+ channels in the membrane rather than in the pore, protection of site 1583 from MTS-EA by BTX would constitute evidence that the reactive sulfhydryl does not face the pore.

BTX was added to the electrode solution at a final concentration of 5 μM when inside-out and when outside-out patches were used. BTX binding was brought about by applying a series of 3-ms pulses at 100 Hz from −120 mV to −20 mV. The number of pulses required to get complete BTX binding varied from patch to patch, and was generally between 1000 and 20,000. Fig. 10 *A* shows a current trace elicited by a pulse from −140 mV to −20 mM in an inside-out patch after 5000 pulses with 5 μM BTX in the electrode solution. As expected, there was neither fast nor slow inactivation over the duration of the 9-s long pulse. (Recall that in non-BTX-modified V1583C, slow inactivation is nearly complete after 2 s.)

For the modification experiments with BTX present, we applied pulses until the fraction of the total channels modified by BTX was between 30 and 50%. This way, the modification of the non-BTX-bound fraction could serve as an internal control with which to compare the effects of MTS-EA on the BTX-modified fraction. Fig. 10 *B* shows, superimposed, a series of traces elicited during successive 1.0-s exposures of an inside-out patch to 1.5 mM MTS-EA at −100 mV from a holding potential of −130 mV. The inactivating component reflects the non-BTX-bound fraction, and MTS-EA appears to have its normal effect: a progressive decline in the peak current. By contrast, the non-inactivating component, reflecting the BTX-bound fraction, shows no change over the course of the modification reaction, suggesting that BTX might completely protect site 1583 from internal modification.

Fig. 10 *C* shows the modification time course for the experiment shown in Fig. 10 *B*, evaluated in two different ways. The filled circles represent the peak current in the test pulse, measured between 0 and 4 ms after depolarization. The open circles represent the steady-state current, evaluated between 2 and 4 ms (when the non-BTX-bound fraction had inactivated), normalized to the peak current between 0 and 4 ms before modification. The filled circles represent modification of the total, while the open circles represent modification of the BTX-bound fraction only. The steady-state current (reflecting the BTX-bound fraction) is not significantly altered, despite the fact that the non-BTX-bound fraction is modified with a rate (158.8 $M^{-1}\,s^{-1}$) similar to the rate for internal modification at −100 mV measured in the absence of BTX (Fig. 5 *B*, 177 ± 26 $M^{-1}\,s^{-1}$). Moreover, the two time courses converge at a plateau of ~25%, indicating that the non-BTX-bound fraction is essentially completely modified.

Fig. 10 *D* shows a similar experiment conducted for external modification of an outside-out patch. As in the preceding experiment, the electrode solution contained 5 μM BTX, and a series of pulses was administered to bring the fraction of BTX-bound channels to between 30 and 50%. The outside-out patch was subjected to 1.0-s exposures to external 1.5 mM MTS-EA at −100 mV. As was the case for internal modification, only the non-BTX-bound fraction shows the progressive current decay associated with MTS-EA modification. The BTX-bound fraction appears unaffected by the exposures to MTS-EA. The modification time courses shown in Fig. 10 *E* are analogous to those shown in Fig. 10 *C* and show essentially the same result. The non-BTX-bound fraction was modified with a rate (163 $M^{-1}\,s^{-1}$) similar to the modification rate for external MTS-EA at −100 mV measured with no BTX present (Fig. 5 *B*, 146 ± 17 $M^{-1}\,s^{-1}$). The two time courses converge to the same value, 31%, which reflects the unaffected BTX-bound fraction.

To rule out the possibility that the voltage-dependence of the modification reaction is dramatically shifted so that modification does not occur at −100 mV, but might occur at other voltages, we placed the patches under continuous MTS-EA perfusion after the non-BTX-bound fraction was fully modified, and alternated a few times between a holding potential of −140 mV and −20 mV (roughly a minute at each voltage). There was no effect on the BTX-bound channels, neither in inside-out nor in outside-out patches.

Another possibility is that the BTX-bound fraction is modified by MTS-EA, but that the bound BTX prevents the associated reduction in the peak current. The easiest way to test this possibility would be to wash out the BTX and show that normal V1583C current remained. However, BTX binding is essentially irreversible, and in these modification reactions the BTX was kept in the electrode solution, so this experiment was not an option. Instead, we used a different strategy. Both inside-out and outside-out patches with 5 μM BTX in the electrode solution were subjected to complete MTS-EA modification, thereby eliminating the Na^+ cur-

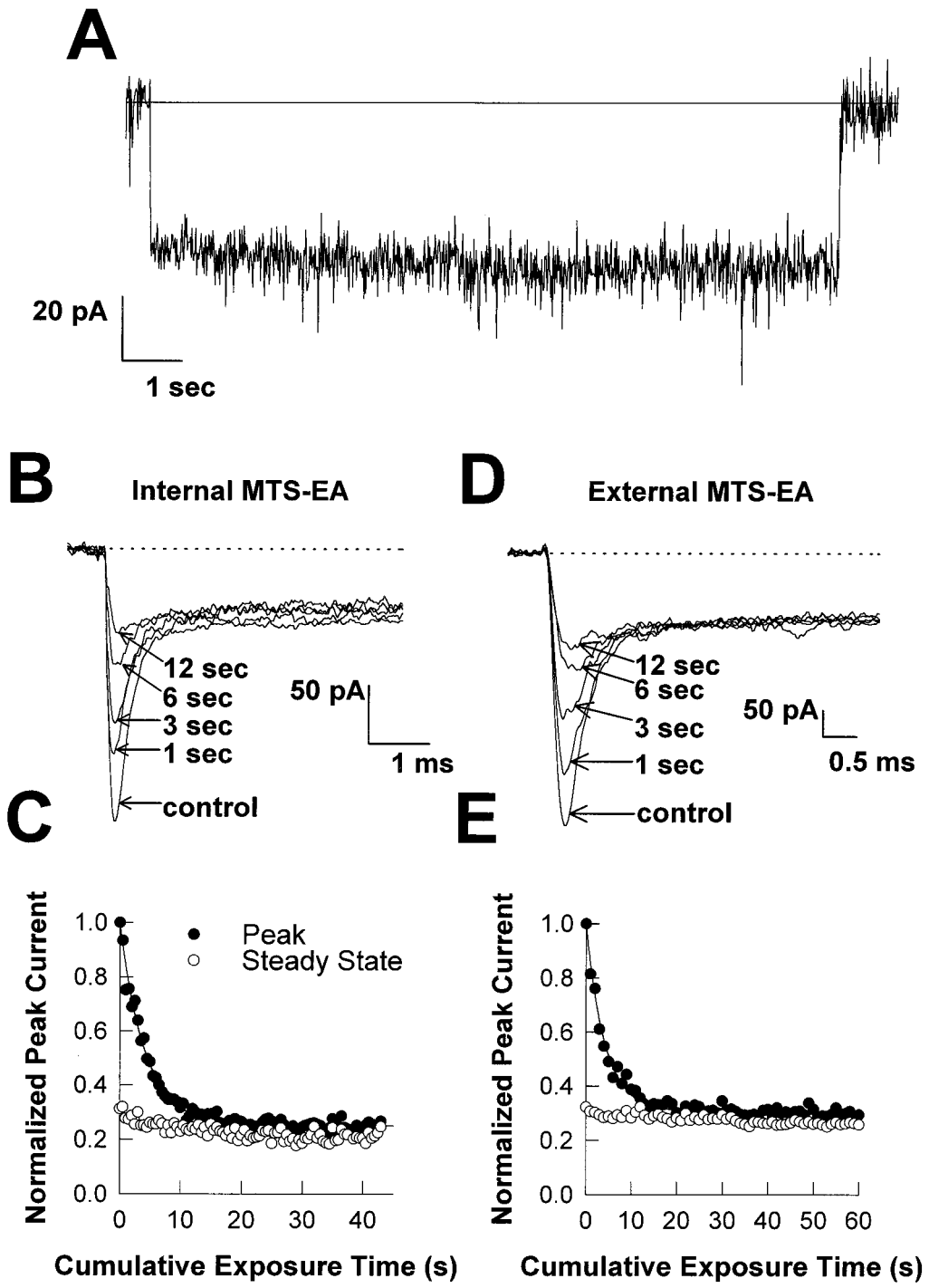

FIGURE 10 Batrachotoxin binding prevents the modification reaction. (*A*) An inside-out patch with 5 μM BTX in the electrode solution was subjected to 20,000 3-ms pulses from −120 mV to −20 mV to allow complete BTX binding. A 10-s pulse from −140 to −20 mV shows a loss of both fast and slow inactivation. (*B*) Rapid pulsing from −120 mV to −20 mV was applied to an inside-out patch containing 5 μM BTX in the electrode solution until a significant fraction of the macroscopic current showed the loss of inactivation characteristic of BTX binding. The patch was then subjected to a series of 0.5-s exposures to 1.5 mM internal MTS-EA at −100 mV. Successive traces showed a reduction in the non-BTX-bound fraction, with no change in the BTX-bound fraction. (*C*) Peak currents from traces elicited by the experiment in (*B*) were evaluated over an interval of 0–4 ms after depolarization (*filled circles*) or 2–4 ms after depolarization (*open circles*), and plotted against cumulative exposure time. The time constant of the modification time course was 4.2 s, with a plateau of 25%. (*D*) The experiment described in (*B*) was performed on an outside-out patch, with 5 μM BTX in the electrode solution. (*E*) Peak currents from a 0–4-ms window (*filled circles*) or 2–4-ms window (*open circles*) from the traces elicited in the experiment in (*D*) were plotted against cumulative exposure time (τ = 4.1 s, plateau = 31%).

rent, before beginning the rapid pulsing needed to promote BTX-binding. After complete MTS-EA modification occurred we applied thousands of pulses to see if we could resuscitate the sodium current with BTX, which would indicate that when BTX and MTS-EA are both bound to the channel, conduction occurs as it does in BTX-bound channels not modified by MTS-EA.

No matter how may pulses we administered (up to 60,000), we were never able to bring sodium current back from MTS-EA modification, suggesting (though not proving conclusively) that BTX binding and MTS-EA modification do not result in a conducting channel. We propose that BTX binding and MTS-EA modification are mutually exclusive, because the BTX molecule sterically protects site 1583 from MTS-EA modification.

DISCUSSION

The major results of this study are that the rate of modification of V1583C by MTS-EA depends upon the state of a rapid conformational change coupled to fast inactivation and the position of the slow-inactivation gate; and that the modified thiol of V1583C is likely to be at ~15–25% of the way into the electric field, to face away from the pore, and to lie in close proximity to the BTX receptor.

Site 1583 and fast inactivation

Experiments on the voltage-dependence of V1583C accessibility demonstrated that accessibility increases of ~10–20-fold are associated with a rapid conformational change, with a $V_{1/2}$ of −87 mV, which is between the $V_{1/2}$ of steady-state voltage-dependent availability (−100 mV) and $G(V)$ (−33 mV). This result suggests that the conformational change being tracked is identical neither to channel opening nor to fast inactivation. However, the conformational change does appear to be influenced by the part of the fast-inactivation mechanism contributed by the III-IV linker, because the $V_{1/2}$ shifts by ~26 mV in the depolarizing direction when fast inactivation is disrupted by introducing the IFM1303QQQ mutant, without substantial changes in the $R_{max(int)}$, $R_{min(int)}$, or $z\delta$. The best explanation for this result is that the underlying conformational change is coupled to fast inactivation, so that when the channel cannot fast-inactivate, more depolarization is required to induce the coupled conformational change.

One possibility is that the conformational change reflects a rearrangement in the S6 region required for fast inactivation. This is unlikely, however, because the conformational change does not begin in full force until nearly all of the channels are fast-inactivated. Another possibility is that the conformational change is an early step required for slow inactivation. This, too, is unlikely because loss of fast inactivation generally shifts the voltage-dependence of slow inactivation in the hyperpolarizing direction, whereas the rapid conformational change tracked by site 1583 accessibility shifts in the depolarizing direction with the loss of fast inactivation.

The rapid movement might represent a conformational change along the activation pathway required for, but not identical to, channel opening. Because activation and fast inactivation are believed to be coupled, this would explain both the intermediate voltage-dependence of the transition and the fact that its voltage-dependence is affected by disrupting inactivation. In both *Streptomyces* K^+ channels and *Shaker* K^+ channels, movements of S6 segments or their homologs are thought to be related to channel activation gating, lending some plausibility to this hypothesis (Liu et al., 1997; Perozo et al., 1999). Without more detailed information about site 1583 and neighboring residues, however, it is impossible to say with any certainty what the nature of this rapid conformational change is.

Site 1583 and slow inactivation

We also showed that the accessibility of site 1583 is reduced during prolonged depolarization, and that the change in accessibility has the same time-dependence and voltage-dependence as slow inactivation. Although this finding demonstrates that there is a movement correlated with slow inactivation in the vicinity of V1583C, by itself it does not shed much light on the nature and extent of the conformational change, or on the structural basis of slow inactivation.

However, in conjunction with data from other studies, our findings do permit some mechanistic interpretation. First, numerous studies have found that there are at least two distinct slow-inactivated states through which channels pass, as evidenced by multiple phases of recovery from long conditioning pulses, with recovery time constants ranging from hundreds of milliseconds to seconds (Cummins and Sigworth, 1996; Hayward et al., 1997). The slow-inactivated state from which recovery is fastest appears to be identical to the first slow-inactivated state through which channels pass during a prolonged depolarization. (This state has been given the name "intermediate inactivation" (I_m) in some studies (Balser et al., 1996).) Because accessibility of site 1583 declines with the time course of entry to the slow-inactivated state populated earliest during depolarization, the conformational change tracked by the modification reaction is likely to be entry to the I_m state.

Previous studies have identified I_m-associated movements near the outer mouth of the pore (Benitah et al., 1999), and have identified a residue in the pore region, W402, which appears to be involved in the early steps of slow inactivation (Balser et al., 1996). In addition, external Na^+ ions, but not internal Na^+ ions, inhibit the development of slow inactivation (Townsend and Horn, 1997), lending some support to the outer mouth hypothesis. Finally, C-type inactivation of *Shaker* K^+ channels, in many ways analo-

gous to slow inactivation of Na^+ channels, involves a constriction of the outer mouth of the pore (Liu et al., 1996; Loots and Isacoff, 1999).

Our data suggest that there is some I_m-associated movement that affects the accessibility of a site in the middle of IVS6, probably in a region near the inner vestibule of the channel. This result is also consistent with the finding that many mutations in S6 regions either enhance or destabilize slow inactivation (Hayward et al., 1997; Takahashi and Cannon, 1999; Wang and Wang, 1997; Wright et al., 1998). One hypothesis consistent both with these results and with the results that point to involvement of the outer mouth is that slow inactivation is a delocalized conformational change involving concerted movements in more than one area of the channel, including the outer mouth of the pore and the inner vestibule.

To test this hypothesis, we attempted a more extensive survey of residues in segment IVS6 near V1583, but the residues we tested were not useful either because there was no effect of modification reagents on the ionic current (L1580C), because gating was significantly altered (I1581C), or because the modification rates were too slow to permit the brief-exposure-based methods used in our study (V1582C).

Though our results do not give detailed information about the molecular mechanism of slow inactivation, the discovery of a conformational marker for slow inactivation may be useful in studying the relation of slow inactivation to other gating processes and to pharmacological agents. For example, one group has proposed that lidocaine dramatically accelerates entry to a slow-inactivated state, thereby explaining the slow recovery of Na^+ channel availability after relatively brief depolarizations in the presence of lidocaine (Kambouris et al., 1998). Using a conformation marker such as the one developed here would enable direct determination of whether slowly recovering channels are slow-inactivated or not.

The location of site 1583

Establishing the precise location of site 1583 relative to the membrane and to the pore is impossible without more detailed structural information. However, our data do provide a basis for proposing whether or not site 1583 faces the pore and about the location of site 1583 within the membrane.

The first finding is that only MTS-EA, and not MTS-ET, -ES, or -HE, can modify the channel. Both MTS-ET and MTS-ES are permanently charged and do not readily cross membranes (Holmgren et al., 1996), and both are larger than MTS-EA (-ET has a quaternary substituted amine, and -ES has an SO_3^- group, while -EA is a primary amine). MTS-HE, however, is a primary alcohol, and so is uncharged and of roughly the same size as MTS-EA. If the reason why MTS-ES and MTS-ET cannot modify V1583C were purely because of hydrophobicity, then MTS-HE should be able to react. Because it does not, it is unlikely that the differential ability of MTS-EA to modify V1583C is based solely on its hydrophobicity, though that might be a contributing factor. Because MTS-HE is also of roughly the same size as MTS-EA, it is unlikely that size alone is the determining factor either.

One possibility is that the ability of MTS-EA to exist in a charged and uncharged form gives it the properties required for modifying V1583C: perhaps it exists in a protonated form in one segment of the pathway to the reaction site, and in an unprotonated form for the rest of the pathway. Lidocaine, another titratable amine, has effects on Na^+ channels that are distinct from those induced by uncharged derivatives, such as benzocaine, and those induced by permanently charged derivatives, such as QX-314 (Hille, 1977). Still another possibility is that some other chemical property of MTS-EA endows it with the ability to react with V1583C.

The intrinsic voltage-dependence of the modification reaction gives a $z\delta$ of between 0.16 and 0.26 from the inside. Though it is difficult to estimate the actual electrical distance to the reactive site on the basis of these values, it is likely that it lies somewhere in the electric field, most probably closer to the inside. The failure to observe intrinsic electric field-dependence when MTS-EA was applied externally raises the possibility that the pathway taken by external MTS-EA does not involve movement of a charged form of the reagent through the electric field. Instead, external MTS-EA might lose a proton and traverse partway through the membrane to a membrane-facing reactive site. If site 1583 is indeed in the electric field, as our data from internal modification suggest, then internally applied MTS-EA might proceed to the reactive site in a charged form for part of the way, and an uncharged form for the remainder of the pathway, most likely through the membrane. This hypothesis is consistent with the idea that the reactive site faces the membrane, while a portion of the internal pathway is aqueous.

Further support for the idea that the site does not face the pore comes from the data on the modification rate with TEA present. Because internal TEA binds at an electrical distance of ~50%, and occupies the pore 65% of the time at 20 mM and +25 mV, it is unlikely that it would have no effect at all on the rate of modification from the outside if the path taken by the reagent involves the pore. Because the modification rate from either side was totally unaffected by the presence of TEA within the pore, it is likely that the pore does not comprise a significant portion of the pathway to the reactive site from either direction.

The final piece of evidence consistent with a membrane-facing location for the reactive site is the fact that BTX gives complete protection from MTS-EA applied from either side of the membrane. The protection from modification occurred not only at −100 mV, but across the voltage

range of gating, suggesting that the protection was not a simple shift in the state-dependence of the modification rate. These data are consistent with at least two possibilities: 1) either the prevention of modification is an allosteric effect, i.e., BTX might induce a channel state whose conformation is different from any of the states occupied without toxin present, and in which site 1583 is buried; or 2) site 1583 comprises part of the BTX receptor, so that binding of BTX physically blocks access of MTS-EA to the reactive site. In light of the mutagenesis data that have identified residues in the immediate vicinity of site 1583 as the probable BTX receptor, and in light of the high degree of BTX protection from modification, we favor the second possibility as the most likely one. And because BTX is believed to bind at the membrane-channel interface, this second possibility is consistent with a membrane-facing location of the reactive site.

The relation of BTX action to inactivation gating

Although the information derived from our experiments is too local to support any conclusions about the molecular mechanisms of BTX action or slow inactivation, it does, in the context of previous studies, permit us to generate hypotheses about the mechanism of BTX action and slow inactivation that will require further testing.

BTX shifts the voltage-dependence of activation in the hyperpolarizing direction, prevents all forms of inactivation, and slows deactivation (Khodorov, 1985). Moreover, it binds only with repetitive depolarizations; it will not bind to resting channels or to channels held at depolarized potentials (Tanguy and Yeh, 1991). These findings are consistent with the idea that BTX preferentially binds to, and greatly stabilizes, open sodium channels.

Mutagenesis experiments have identified two clusters of amino acid residues that are critical for BTX action, one in the middle of segment IS6 (I433, N434, and L437; Wang and Wang, 1998) and one in the middle of segment IVS6 (F1579 and N1584; Linford et al., 1998; Wang and Wang, 1999). Photoaffinity labeling and antibody mapping experiments on BTX have localized binding to IS6 (Trainer et al., 1996), and interactions between local anesthetic binding (in IVS6) and BTX action (Linford et al., 1998) have provided independent evidence that segment IVS6 contributes to the BTX binding site as well. Current structural hypotheses about BTX binding have integrated all of these findings and involve a binding site partly in IS6 and partly in IVS6 at the domain interface rather than in the inner vestibule formed by the S6 segments (Wang and Wang, 1999).

Moving from this structural description of the binding site to the mechanism of open-state stabilization by BTX (hyperpolarizing shift of activation, slowing of deactivation, prevention of inactivation) has been difficult because the roles played by S6 segments in gating are not completely understood. Our results may shed some light on this problem. We have found that there are two conformational changes that occur in the vicinity of segment IVS6, one a rapid change indirectly coupled to fast inactivation and one closely tied to slow inactivation. Because BTX appears to bind at a place where these conformational changes are occurring, it is plausible that BTX inhibits the movements at these sites associated with the gating changes.

The way BTX might inhibit these movements is by generating an intersubunit molecular bridge between the two portions of its binding sites on segments IS6 and IVS6 (brought in proximity to each other when the channel opens), thereby preventing the relative movements of these segments necessary for inactivation gating and deactivation. Support for this hypothesis comes from findings in K^+ channels: an intersubunit metal bridge between S6 segments in *Shaker* K^+ channels causes open-state stabilization, presumably by stabilizing the open conformation and inhibiting the relative movements of S6 segments that occur during deactivation (Holmgren et al., 1998). The *Shaker* residue at which this bridge forms, V476, is homologous to V1583 in rSkM1 according to sequence alignment (Jan and Jan, 1990). BTX and other site 2 neurotoxins may constitute natural analogs of the artificially induced open-state stabilization seen in the metal-bound K^+ channels.

These hypotheses about BTX action have ramifications for the nature of the conformational changes we observed at site 1583. If restriction of relative movements of IS6 and IVS6 disrupts inactivation gating, it is plausible that inactivation gating may partly consist of such movements. This hypothesis accords particularly well with what is known about the structural basis of slow inactivation: many of the mutations that affect slow inactivation have been localized either to IS6 or IVS6, with the others either in S5 segments or in the pore-region, which links S5 and S6. A rearrangement of the S6 segments with an associated movement in the adjacent pore-region would account for all the major findings about the structural basis of slow inactivation.

We thank Dr. Ging Kuo Wang and Dr. John W. Daly for providing us with batrachotoxin.

This work was supported by National Institutes of Health Grant RO1-AR42703 (to S.C.C.) and a grant from the Harvard Mahoney Neuroscience Institute (to V.V.).

REFERENCES

Balser, J. R., H. B. Nuss, N. Chiamvimonvat, M. T. Perez-Garcia, E. Marban, and G. F. Tomaselli. 1996. External pore residue mediates slow inactivation in μ1 rat skeletal muscle sodium channels. *J. Physiol.* 494:431–442.

Benitah, J., Z. Chen, J. R. Balser, G. F. Tomaselli, and E. Marban. 1999. Molecular dynamics of the sodium channel pore vary with gating: interactions between P-segment motions and inactivation. *J. Neurosci.* 19:1577–1585.

Cannon, S. C., and S. M. Strittmatter. 1993. Functional expression of sodium channel mutations identified in families with periodic paralysis. *Neuron.* 10:317–326.

Cha, A., P. C. Ruben, A. L. George, Jr., E. Fujimoto, and F. Bezanilla. 1999. Voltage sensors in domains III and IV, but not I and II, are immobilized by Na^+ channel fast inactivation. *Neuron.* 22:73–87.

Chen, C. F., and S. C. Cannon. 1995. Modulation of Na^+ channel inactivation by the β_1 subunit: a deletion analysis. *Pflügers Arch.* 431: 186–195.

Cummins, T. R., and F. J. Sigworth. 1996. Impaired slow inactivation in mutant sodium channels. *Biophys. J.* 71:227–236.

Derra, E., A. Alekov, N. Mitrovic, F. Lehmann-Horn, and H. Lerche. 1999. Voltage-dependent accessibility of the IV/S6 segment of the Na^+ channel. *Biophys. J.* 76:194*a*. (Abstr).

Hayward, L. J., R. H. Brown, Jr., and S. C. Cannon. 1996. Inactivation defects caused by myotonia-associated mutations in the sodium channel III-IV linker. *J. Gen. Physiol.* 107:559–576.

Hayward, L. J., R. H. Brown, Jr., and S. C. Cannon. 1997. Slow inactivation differs among mutant Na^+ channels associated with myotonia and periodic paralysis. *Biophys. J.* 72:1204–1219.

Hille, B. 1977. Local anesthetics: hydrophilic and hydrophobic pathways for the drug-receptor reaction. *J. Gen. Physiol.* 69:497–515.

Holmgren, M., Y. Liu, Y. Xu, and G. Yellen. 1996. On the use of thiol-modifying agents to determine channel topology. *Neuropharmacology.* 35:797–804.

Holmgren, M., K. S. Shin, and G. Yellen. 1998. The activation gate of a voltage-gated K^+ channel can be trapped in the open state by an intersubunit metal bridge. *Neuron.* 21:617–621.

Kambouris, N. G., L. A. Hastings, S. Stepanovic, E. Marban, G. F. Tomaselli, and J. R. Balser. 1998. Mechanistic link between lidocaine block and inactivation probed by outer pore mutations in the rat μ1 skeletal muscle sodium channel. *J. Physiol.* 512:693–705.

Kellenberger, S., T. Scheuer, and W. A. Catterall. 1996. Movement of the Na^+ channel inactivation gate during inactivation. *J. Biol. Chem.* 271: 30971–30979.

Khodorov, B. I. 1985. Batrachotoxin as a tool to study voltage-sensitive sodium channels of excitable membranes. *Prog. Biophys. Mol. Biol.* 45:57–148.

Jan, L. Y., and Y. N. Jan. 1990. A superfamily of ion channels. *Nature.* 345:672.

Liman, E. R., J. Tytgat, and P. Hess. 1992. Subunit stoichiometry of a mammalian K^+ channel determined by construction of multimeric cDNAs. *Neuron.* 9:861–871.

Linford, N. J., A. R. Cantrell, Y. Qu, T. Scheuer, and W. A. Catterall. 1998. Interaction of Batrachotoxin with the local anesthetic receptor site in transmembrane segment IVS6 of the voltage-gated sodium channel. *Proc. Natl. Acad. Sci. USA.* 95:13947–13952.

Liu, Y., M. Holmgren, M. E. Jurman, and G. Yellen. 1997. Gated access to the pore of a voltage-dependent K^+ Channel. *Neuron.* 19:175–184.

Liu, Y., M. E. Jurman, and G. Yellen. 1996. Dynamic rearrangement of the outer mouth of a K^+ channel during gating. *Neuron.* 16:859–867.

Loots, E., and E. Y. Isacoff. 1999. protein rearrangements underlying slow inactivation of the *Shaker* K^+ channel. *J. Gen. Physiol.* 112:377–389.

McClatchey, A. I., S. C. Cannon, S. A. Slaugenhaupt, and J. F. Gusella. 1993. The cloning and expression of a sodium channel beta 1-subunit cDNA from human brain. *Hum. Mol. Genet.* 2:745–749.

McPhee, J. C., D. S. Ragsdale, T. Scheuer, and W. A. Catterall. 1994. A mutation in segment IVS6 disrupts fast inactivation of sodium channels. Proc. Natl. Acad. Sci. USA. 91:12346–12350.

McPhee, J. C., D. S. Ragsdale, T. Scheuer, and W. A. Catterall. 1995. A critical role for transmembrane segment IVS6 of the sodium channel alpha subunit in fast inactivation. *J. Biol. Chem.* 270:12025–12034.

O'Leary, M. E., and R. Horn. 1994. Internal block of human heart sodium channels by symmetrical tetra-alkylammoniums. *J. Gen. Physiol*. 104: 507–522.

Perozo, E., D. M. Cortes, and L. G. Cuello. 1999. Structural rearrangements underlying K^+-channel gating. *Science.* 285:73–79.

Ragsdale, D. S., J. C. McPhee, T. Scheuer, and W. A. Catterall. 1994. Molecular determinants of state-dependent block of Na^+ channels by local anesthetics. *Science.* 265:1724–1728.

Takahashi, M. P., and S. C. Cannon. 1999. Enhanced slow inactivation by V445M: a sodium channel mutation associated with myotonia. *Biophys. J.* 76:861–868.

Tanguy, J., and J. Z. Yeh. 1991. BTX modification of Na channels in squid axons. *J. Gen. Phys.* 97:499–519.

Todt, H., S. C. Dudley, Jr., J. W. Kyle, R. J. French, and H. A. Fozzard. 1999. Ultra-slow inactivation in μ1 Na^+ channels is produced by a structural rearrangement of the outer vestibule. *Biophys. J.* 76: 1335–1345.

Townsend, C., and R. Horn. 1997. Effect of alkali metal cations on slow inactivation of cardiac Na^+ channels. *J. Gen. Physiol.* 110:23–33.

Trainer, V. L., G. B. Brown, and W. A. Catterall. 1996. Site of covalent labeling by a photoreactive batrachotoxin derivative near transmembrane segment IS6 of the sodium channel α subunit. *J. Biol. Chem.* 271:11261–11267.

Vedantham, V., and S. C. Cannon. 1998. Slow inactivation does not affect movement of the fast inactivation gate in voltage-gated Na^+ channels. *J. Gen. Physiol.* 111:83–93.

Vedantham, V., and S. C. Cannon. 1999. The position of the fast-inactivation gate during lidocaine block of voltage-gated Na^+ channels. *J. Gen. Physiol.* 113:7–16.

Wang, S., and G. K. Wang. 1997. A mutation in segment I-S6 alters slow inactivation of sodium channels. *Biophys. J.* 72:1633–1640.

Wang, S., and G. K. Wang. 1998. Point mutations in segment I-S6 render voltage-gated Na^+ channels resistant to batrachotoxin. *Proc. Natl. Acad. Sci. USA.* 95:2653–2658.

Wang, S., and G. K. Wang. 1999. Batrachotoxin-resistant Na^+ channels derived from point mutations in transmembrane segment D4–S6. *Biophys. J.* 76:3141–3149.

West, J. W., D. E. Patton, T. Scheuer, Y. Wang, A. L. Goldin, and W. A. Catterall. 1992. A cluster of hydrophobic amino acid residues required for fast Na^+-channel inactivation. *Proc. Natl. Acad. Sci. USA.* 89: 10910–10914.

Wright, S. N., S. Wang, and G. K. Wang. 1998. Lysine point mutations in Na^+ channel D4–S6 reduce inactivated channel block by local anesthetics. *Mol. Pharmacol.* 54:733–739.

Yang, N., A. L. George, Jr., and R. Horn. 1996. Molecular basis of charge movement in voltage-gated sodium channels. *Neuron.* 16:113–122.

Yang, N., and R. Horn. 1995. Evidence for voltage-dependent S4 movement in sodium channels. *Neuron.* 15:213–218.